ADVANCED ELECTRONIC MATERIALS Open Access
www.advelectronicmat.de

Polycaprolactone-Based Zinc Ink for High Conductivity Transient Printed Electronics and Antennas

*Carol L. Baumbauer, Anupam Gopalakrishnan, Madhur Atreya, Gregory L. Whiting, and Ana C. Arias**

Distributed sensors and electronics can be used in agriculture to optimize crop management and improve environmental outcomes. Electronic devices in these outdoor spaces require medium to long range (>1m) wireless communication of data over several weeks or months, which in turn requires high conductivity (1×10^5 Sm^{-1}) antennas. Printed bioinert or ecoresorbable conductors, comprising carbon, magnesium, or zinc fillers, typically exhibit conductivity on the order of 10–1000 Sm^{-1} and lifetimes from a few hours to a few days. A print-based fabrication process for chemically treated zinc traces, which achieves conductivity of up to 6×10^5 Sm^{-1} is reported here. The ink formulation uses a non-water-soluble soil biodegradable polycaprolactone binder. The ink and printing processes reported here led to stable conductive traces that are used in ultra high frequency radio frequency identification (UHF-RFID) folded dipole antennas operating at 915 MHz. The conductivity of the printed traces is maintained for over 70 days in ambient environments when traces are protected by a biodegradable beeswax encapsulation layer.

1. Introduction

Transient electronics are designed to operate for a specific amount of time before degrading in their environment, leaving minimal harmful byproducts. This is a growing field of research that provides a sustainable alternative to conventional electronics through eco-friendly materials and processing techniques that reduce electronic waste. The transient nature of these devices confers a significant advantage since they do not require servicing or retrieval when they are longer needed. These unique characteristics could enable deployment of electronic devices in environments with challenging or inconvenient access, such as inside a human body, or distributed within the environment, such as throughout a forest or an agricultural field. Significant progress has been achieved for medical applications with the development of electronic components such as sensors, supercapacitors, and microresonators that are biodegradable or bioresorbable.[1–6] Similar technologies could also revolutionize environmental and agricultural sensing.[7] However, environmental applications present a different set of challenges than medical applications: the devices typically need to last for months rather than days, function in a broader range of temperature and humidity conditions, degrade in uncontrolled environments, and communicate their data over distances of a few meters, rather than centimeters.[7] Electrical conductors are a key enabling constituent of biodegradable electronic systems, as they form both the interconnects between sensors and integrated circuits, as well as the antennas for power and data transmission. While moderate conductivity is acceptable for interconnects carrying small, low frequency currents, higher conductivity is needed for radio frequency antennas designed to transmit data over distances more than a few centimeters.

Development of transient wireless communication systems has focused on near field communication (NFC), which operates in the 13.5 MHz band and has a maximum transmission distance of 4 cm.[8,9] Demonstrations of bioresorbable RF antennas have shown wireless links of a few 10's of cm[6,10] but in environmental or agricultural applications, longer read ranges are critical. In order to achieve a system with long read range, antennas with low resistive losses are needed. The impact of low conductivity on the performance of antennas designed for the 0.8–1GHz range was previously studied as printed silver (screen and inkjet) radio frequency identification (RFID) tags became widespread.[11–13] These results give lower bounds on acceptable conductivity of printed antennas. The required trace conductivity depends on the application, the antenna design and the trace thickness. Shahpari reports a comparison of dipole antennas fabricated with silver printed traces with conductivity varying from 1×10^3 to 1×10^7 Sm^{-1}. Antennas fabricated with trace conductivity of 1×10^3 Sm^{-1} show radiation efficiency 40% lower than those fabricated with conductivity traces of 1×10^7 Sm^{-1}. The report further shows that antennas fabricated with trace

C. L. Baumbauer, A. C. Arias
University of California Berkeley
Berkeley, CA USA
E-mail: acarias@berkeley.edu
A. Gopalakrishnan, M. Atreya, G. L. Whiting
University of Colorado Boulder
Boulder, CO USA

The ORCID identification number(s) for the author(s) of this article can be found under https://doi.org/10.1002/aelm.202300658

DOI: 10.1002/aelm.202300658

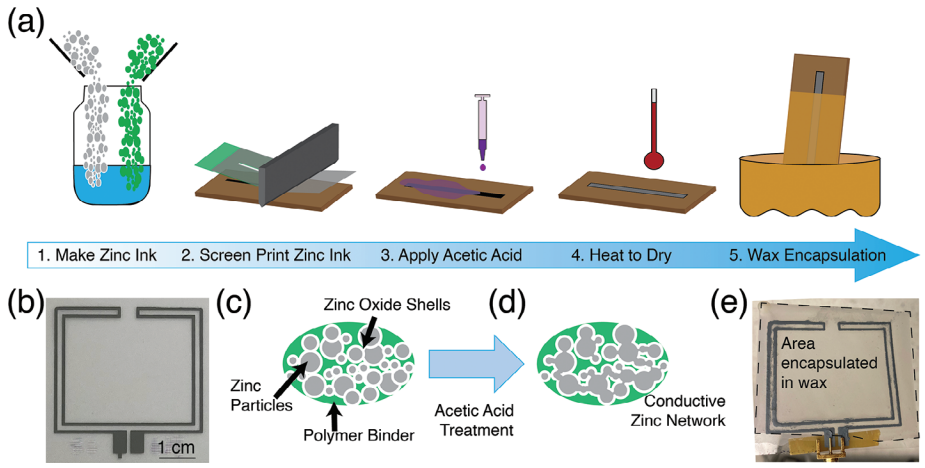

Figure 1. a) The zinc printing and treatment process consists of five major steps: ink formulation, screen printing, acid treatment, drying, and encapsulation. b) An optical image of a folded dipole antenna made of screen printed ink before acid treatment. c) As-printed zinc ink consists of discrete zinc micro particles, each with an oxide shell. This matrix is not conductive. d) After treatment with a solution of acetic acid, which reacts with the oxide layer, a conductive network of zinc is formed. A new passivation layer forms on the outside of the network. e) A treated zinc antenna which has been dip-coated in beeswax to prevent further oxidation of the zinc.

conductivity of 1×10^5 Sm^{-1} present a 5 % reduction in radiation efficiency.[13]. These demonstrations suggest that a conductor with conductivity $>1 \times 10^5$ Sm^{-1} could operate well as an antenna trace.

Conducting polymers and most forms of conductive carbon yield traces with conductivity between 10–1000 Sm^{-1}.[14] Inks composed of a metal filler and a polymer binder show conductivity ranging from 1000–500 000 Sm^{-1}. In these inks, the metal contributes to the material electrical conductivity whereas the polymeric binder influences the in properties and determines the mechanical and stability properties of the final conducting trace. Eco- or bio-resorbable metal fillers include magnesium, iron, zinc (Zn), molybdenum, tungsten, and their alloys, which react in aqueous solutions and form metal hydroxides and hydrogen gas.[5] Previous studies have used zinc to create conductive ($>1 \times 10^4$ Sm^{-1}) traces using low temperature, solution based fabrication methods that are compatible with a variety of biodegradable substrates[8,10,15–18] Table S1 (Supporting Information) summarizes key parameters of several works using printed zinc traces, such as materials and processes used, resulting conductivity, radio frequency (RF) frequency tested, and lifetime.

The process flow for solution-based deposition of conductive zinc traces is shown in **Figure 1a**. The zinc ink is prepared by combining zinc microparticles with a binder and a solvent. The materials used as binders in biodegradable conductive inks are often water soluble polymers or aliphatic polyesters that break down by hydrolysis of the ester group, sometimes assisted by microbial enzyme activity. In this study, we used polyvinylpyrrolidone (PVP) and polycaprolactone (PCL) as binders. PVP is a water-soluble polymer used in pharmaceuticals, contact lenses, and other household products, and has been demonstrated in the literature as a binder for printed zinc traces.[8,10,16,17,19] PCL is an aliphatic polyester that has seen use in active food-packaging,[20] drug-delivery systems,[21] and other biomedical applications.[22] Degradation of PCL is slow in water due to its hydrophobic nature, but is accelerated in natural environmental conditions such as soils[23] and in the presence of the enzyme lipase.[24]

The zinc ink is deposited on to the substrate using screen printing. Screen printing can be used to pattern thicker layers than those deposited by inkjet printing. In addition screen printing shows reproducible results and can readily be scaled to large areas and large volumes in contrast with stencil-patterned based approaches such as spray coating.[25] Figure 1b shows a screen printed folded dipole antenna.

As deposited, each zinc particle is surrounded by a shell of zinc oxide, hydroxides, and carbonates; therefore, as previously reported, and a printed zinc trace is not conductive as deposited (Figure 1c). Printed zinc traces can be made conductive through chemical processing, photonic sintering, or a combination of the two. Photonic sintering uses a UV laser to heat the zinc particles, melting, and welding them together.[9,16] This can be an effective technique, but it requires specialized, high power UV light sources. Photonic sintering of printed zinc is especially challenging because of the high melting temperature of zinc oxide.[17] Alternatively, chemical treatment with dilute acetic acid dissolves the native passivation layer, exposing the metallic zinc, as previously demonstrated through x-ray studies.[6,8,18] The exposed zinc releases Zn^{2+} ions into solution, some of which are chelated with acetate, and drive self-exchange between zinc in solution and zinc solid. Chemical treatment thus creates a conductive network of zinc particles in contact with each other.[8,10,15,18,26] Figure 1d is a schematic representation of how a conductive network of zinc particles can be formed after the treatment.

The acetic acid treatment is not selective and also affects the binder used in the ink. The treatment solution can dissolve or degrade water soluble binders, which can cause smearing of fine printed features. This issue can be addressed by controlling the amount of acid solution released onto the Zn printed traces using an ink-jet printing technique[10,18] or spray coating,[17] or by leveraging ambient humidity to activate the sintering process.[6] However, inkjet and spray depositions require repeated applications of acetic acid and lead to traces with conductivity between 4×10^4 and 2×10^5 Sm^{-1}. On the other hand, inks made with

non-water-soluble binders are not as easily degraded by the aqueous acetic acid solution, which allows them to be treated with more aggressive chemical processes. Drop casting or dipping are simple, one-step processes which are easily scalable.

Once the acetic acid treatment is completed and the substrates have dried, the Zn traces are encapsulated to prevent loss of conductivity from exposure to oxygen and humidity. Prior reports have shown that the conductivity of unencapsulated printed zinc traces decreases over time as the layer of ZnO_x grows, and that exposure to humid environments accelerates the decrease in conductivity.[18] Previous studies have shown that an encapsulation layer prolonged the conductive lifetime of a printed trace by a factor of about 10.[10] Biodegradable waxes are a promising class of materials for encapsulation of electronics in wet environments such as soils because waxes are highly hydrophobic. Beeswax in particular breaks down slowly, and has been demonstrated as an effective encapsulating layer for more than 12 weeks in soil.[27] Additionally, beeswax has been shown to be an effective barrier to humidity in air for electronic sensors operating at DC and radio frequency conditions.[28,29] Figure 1e shows a completed antenna encapsulated using beeswax.

We used this reliable, long lasting zinc conductor to print antennas that operate in the 902–915 MHz band for ultra high frequency radio frequency identification (UHF-RFID). The antennas were of a compact folded dipole design that we had developed in our previous work.[25]

Here, we performed a direct study of the impact of ink binder and acetic acid treatment conditions on trace conductivity. Additionally, we studied the impact of humidity on trace conductivity for two types of binders with and without encapsulation to characterize the lifetime of antennas fabricated with biodegradable and ecoresorbable materials. We have characterized the RF performance of these antennas using both types of ink formulation with and without encapsulation.

2. Results and Discussion

The zinc ink was optimized for screen printing by selecting solvents for each binder and adjusting the solvent to binder to filler ratios. N-Methyl-2-pyrrolidone (NMP), a high boiling point solvent, was chosen as a solvent for PVP. Inks formulated with NMP at ratios of 30:1:5 (Zn:PVP:NMP) by mass resulted in good printed pattern fidelity, uniform print thickness of 50 μm and long pot life, enabling many screen printing passes before the ink dried in the screen. PCL inks with two different solvents were characterized: NMP giving a direct comparison to PVP inks, and anisole, which provides higher PCL solubility. PCL inks in NMP had a shorter pot life and gelled faster than PCL-anisole inks. The ratio used for PCL inks was 30:1:8 (Zn:PCL:solvent) by mass. No significant solvent dependence in conductivity of printed traces was observed. Printed PCL traces were 30μm thick using both ink formulations. Characteristic profiles of printed PVP and PCL traces are shown in Figure S1 (Supporting Information).

Initial process optimization was done on non-degradable polyethylene terephthalate (PET) in order to focus on the conductor itself. The acetic acid treatment was optimized for PVP-based traces by varying acid concentrations between 9–50% in DI water by volume. During the treatment, 1 mL of acetic acid solution was drop cast to cover the 20 cm^2 substrate, including 320 mm of meandered trace length which includes unprinted substrate area. The solution was applied to the sample and remained on the substrate for times ranging from 30 seconds to 5 minutes. After the exposure time, the acetic acid solution was removed and the substrate was dried in an oven. Printability and conductivity data for the acetic acid treatment are summarized in **Figure 2**. Figure 2a shows optical images of representative samples after 1 and 5 minutes exposures to 9%, 25%, and 50% acetic acid. All 5 minute long acetic acid treatments for PVP resulted in dissolution of the ink binder and degradation of the printed pattern, caused by ink reflow. Further, it is shown that treatments performed with 50% concentration acetic acid solution dissolved the pattern after 1 minute of exposure. Figure 2b shows the conductivity of samples treated with 9% acetic acid for times between 30 seconds and 2 minutes. For 30 second treatments, high sample-to-sample variation was observed (4×10^3 to 7×10^4 Sm^{-1}, N = 3). The conductivity reached a plateau for treatments of one minute or more ($8.5 \pm 1.8 \times 10^4$ Sm^{-1}, N = 4). Because treatments longer than one minute were susceptible to reflow, further optimization used one minute exposure times. Figure 2c shows the conductivity of samples treated for one minute with varying acetic acid concentrations and dried at 70 °C (N ⩾ 3 for each concentration). Acetic acid concentrations of 20% and 25% by volume produced zinc traces with slightly higher conductivity ($2.4 \pm 0.7 \times 10^5$ Sm^{-1}) than 9% concentration ($1.4 \pm 0.5 \times 10^5$ Sm^{-1}).

The dependence of conductivity on drying temperature is shown in Figure 2d. All traces in the study were treated with 9% acetic acid for one minute and dried for 15 min. There is no significant relationship between drying temperature and final trace conductivity. The conductivity of all traces was found to be between 1 and 2×10^5 Sm^{-1}.

PCL-based traces were treated with acetic acid concentrations between 9% and 80% with exposure times varying from 1 to 15 min. All exposure and drying conditions were tested with at least N = 5 samples. Optical images in Figure 2e show that PCL traces do not redissolve during 10 min of treatment with up to 60% acetic acid. Low conductivity and high sample-to-sample variation ($1.3 \pm 0.7 \times 10^5$ Sm^{-1}, N = 5) were observed for PCL-based traces treated for less than one minute, as shown in Figure 2f. The highest and most consistent conductivity was found after 12–13 min of treatment, therefore further optimization used this treatment time. Figure 2g shows the conductivity of PCL-based traces as a function of acetic acid concentration for traces treated for 13 min and dried for 15 min at 45 and 60 °C. Traces treated with low concentrations of acetic acid present low conductivity (1.4×10^5) and high sample-to-sample variability (conductivity ranging from 3.6×10^3 to 2.7×10^5 Sm^{-1}), while those treated with 30%–70% acetic acid show higher conductivity and better reproducibility from sample to sample. The highest trace conductivity was 6.2×10^5 Sm^{-1}, for traces treated with 50% acetic acid and dried at 60 °C. Traces treated with acetic acid concentrations above 70% showed lower conductivity (6.4×10^4 Sm^{-1}). At very high acetic acid concentrations, the acid degrades the PCL binder, leading to poor stability and conductivity of the traces.[30,31] For a given concentration, traces that were dried at higher temperature showed higher conductivity.

The impact of drying temperature on PCL trace conductivity is shown in Figure 2h. Traces treated with 50% and 60% acetic acid for 13 min were dried for 15 min at temperatures ranging from

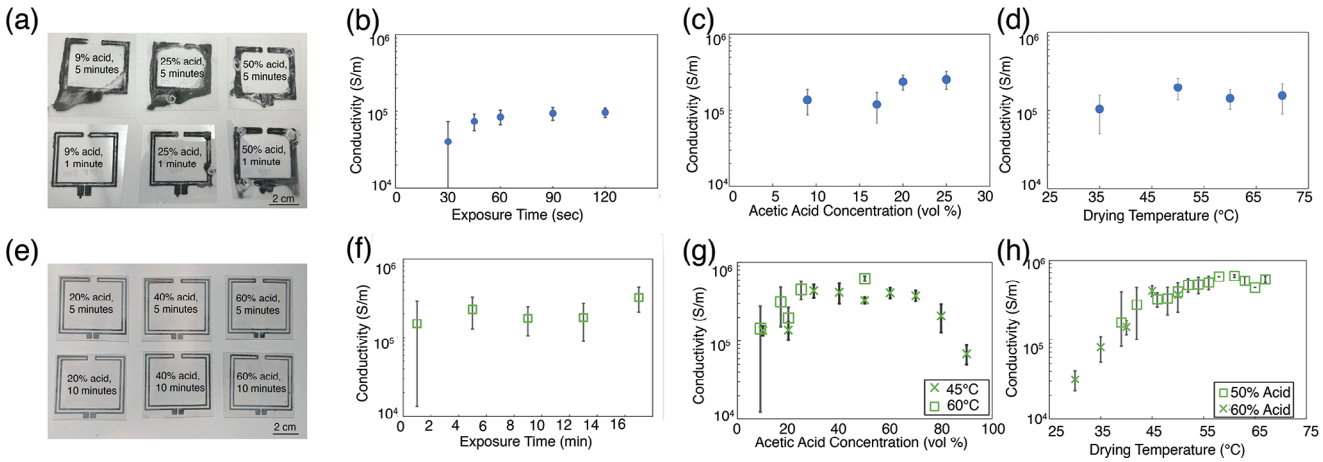

Figure 2. a) Physical condition of PVP-based traces varying acetic acid treatment time and concentration. b) conductivity of printed zinc traces with PVP binder as a function of exposure time to 9% acetic acid solution, and dried at room temperature. c) Conductivity of printed zinc traces with PVP binder as a function of acetic acid concentration, all exposed to acetic acid solution for 1 mi and dried for 15 min at 70 °C. d) Conductivity of printed zinc traces with PVP binder as a function drying temperature, all exposed to 9% acetic acid for 1 min and dried for 15 min. e) Physical condition of PCL-based traces treated with varying acetic acid time and concentration. f) Conductivity of PCL-based zinc traces as a function of exposure time to 50% acetic acid solution and dried at 50C for 15 min. g) Conductivity of PCL-based zinc traces as function of acetic acid concentration, all treated for 13 min and dried at 45 or 60 °C for 15 min. h) Conductivity printed zinc traces with PCL binder as a function of drying temperature, all treated with 50% acetic acid for 13 min.

30 to 67 °C. Increasing temperature from 30 to 60 °C increased conductivity and improved reproducibility. The maximum conductivity of $6.3 \pm 0.25 \times 10^5$ Sm^{-1} was achieved with a drying temperature of 60 °C. The relationship between temperature and conductivity was similar for samples treated with 50% acetic acid and 60% acetic acid.

The relationship between drying temperature and conductivity is consistent with prior reports: Sui and Majee both found that drying at elevated temperatures up to the melting point of the binder increased final trace conductivity, while heating above that point led to lower conductivity.[10,18] Selecting a binder with a high melting point can enable higher temperature curing, and therefore higher conductivity.

Interestingly, PCL traces required heat treatment in order to become conductive. It is possible that the acid treatment and heat treatment serve two different, complementary, functions. The acid treatment removes the oxide shells on the zinc particles, then the heat anneals the bare zinc particles. Measurements of the resistance of PCL-based traces during drying at different temperatures, is shown in Figure S2 (Supporting Information). After acid treatment, the traces have high resistance, and during drying, the resistance decreases by four or five orders of magnitude. Most of this drop happens in the span of a few seconds. This process might be similar to the one developed by Fumeaux et al., which combined chemical dissolution of the zinc oxide shells with photonic annealing of bare zinc traces[17]

In addition, prior studies showed that soaking printed composites of PCL and tungsten in warm water and subsequent vacuum drying at elevated temperatures, yields a significant increase in conductivity.[32] This suggests that the solvent-assisted annealing of PCL, which results in a decrease in the binder's specific volume, could also contribute to the increased conductivity observed here.

SEM studies illustrate the effect of acetic acid treatment on the morphology of Zn-PCL samples, which influences trace conductivity. **Figure 3** shows Zn-PCL traces which were a) untreated; and treated for 13 min with b) 20% acetic acid concentration c) 40% acetic acid concentration d) 60% acetic concentration e) 80% acetic concentration, and dried at 45 °C. Spherical Zn particles and PCL polymer strands are observed in the untreated sample. In Figure 3b, after 20% acetic acid treatment, polymer strands and particles are still observed. In the 40% and 60% treatment (Figure 3c, d), sintering features such as necking are observed, where Zn particles start to form a bridged network. After treatment with 80% acetic acid (Figure 3e), the formation of planar crystalline structures is visible. This may be attributed to excessive dissolution of zinc to form zinc acetate precipitate that might interrupt the conductive zinc network, also contributing to the drop in conductivity that was observed for traces treated with very high concentrations of acetic acid.In addition, the solubility of PCL in acetic acid might result in damage to the traces at these higher concentrations.[30]

In order to take advantage of this transient conductor, it must be compatible with biodegradable substrates. Both PCL- and PVP- based inks were tested on flexible paper substrates, as well as rigid wooden substrates, as shown in **Figure** 4a–e. It can be advantageous to use wooden substrates for sensors, which are intended to be inserted in soil, since the rigid wood provides mechanical support for insertion, as well as being naturally sourced and fully biodegradable. However, many types of wood have a rough, anisotropic surface dominated by grain patterns. The high surface roughness led to gaps in printed traces, significant edge roughness, and poor print quality of fine features. In order to improve printability, a smooth coating of a polymer or wax can be added. Such a coating layer can also serve as back-side encapsulation for the printed trace.

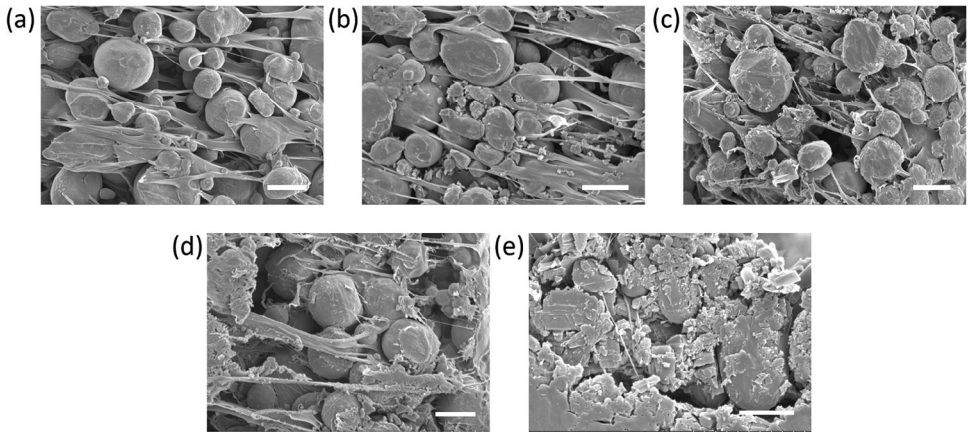

Figure 3. Cross-sectional SEM images of Zn-PCL prints a) before treatment; b,c,d,e) after treating with 20%, 40%, 60%, and 80% acetic acid respectively followed by drying at 45 °C. The scale bars are 5 µm.

PVP traces were tested on paper substrates and wooden substrates coated with beeswax. The sheet resistance of traces on these different substrates were similar (N = 3). PCL traces were tested on paper substrates, wood coated with a PCL film, and on the bioderived, biodegradable polymer poly(3-hydroxybutyrate-co-3-hydroxyvalerate) (PHBV), with no significant difference in electrical properties observed between the substrates, as shown in Figure 4f.

Many biodegradable substrates show low tolerance to elevated temperature. As such, any thermal treatments used (such as for drying) must typically be limited to relatively low temperatures in order to prevent damage to the substrate. However, this restricted thermal processing window for biodegradable substrates does not reduce the achievable conductivity in this case, since temperatures above 60 °C are not used, as this would causing melting of the PCL binder.

The environmental stability of printed Zn traces was characterized over an extended period of time, under different humidity conditions with and without a beeswax encapsulation layer. Encapsulation layers 65 µm thick on each side were applied by dipping the samples in molten wax. **Figure 5** shows the conductivity, σ, of several representative traces over time, with each trace normalized to its own initial conductivity, σ_0. Figure 5a shows samples that were kept in an environmental chamber at 19 °C and 10% relative humidity (RH). Under low humidity, both PVP (blue) and PCL (green) samples remain conductive for over 30 days, and a layer of wax as encapsulation did not improve stability at low humidity.The conductivity of traces, which were exposed

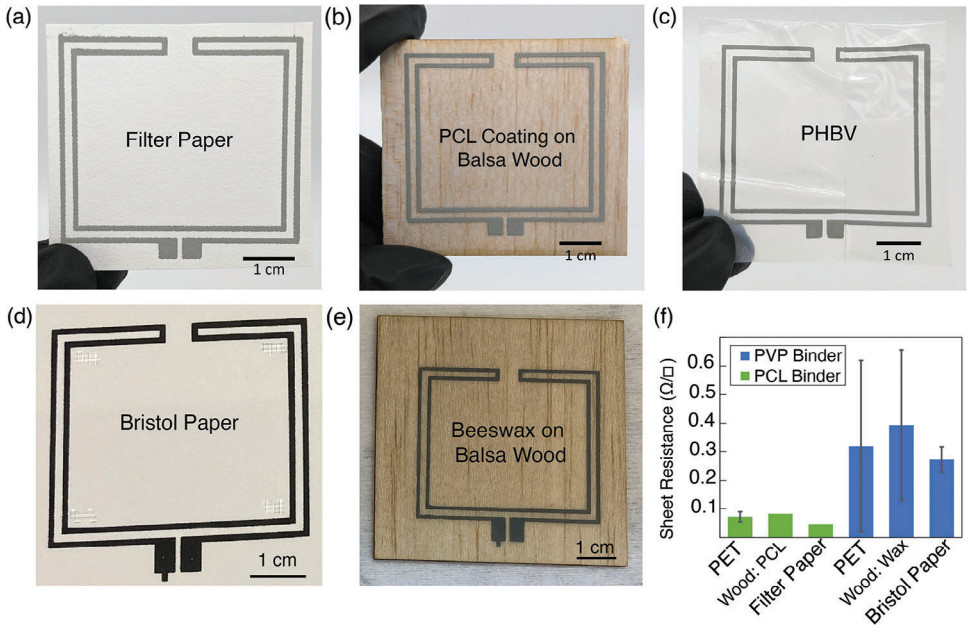

Figure 4. Printed Zn-PCL antennas on a) filter paper; b) PCL-coated balsa wood; c) PHBV sheet. Printed Zn-PVP traces on d) bristol paper, and e) beeswax-coated balsa wood. f) Sheet resistance of PCL and PVP based zinc traces on biodegradable and non-degradable substrates.

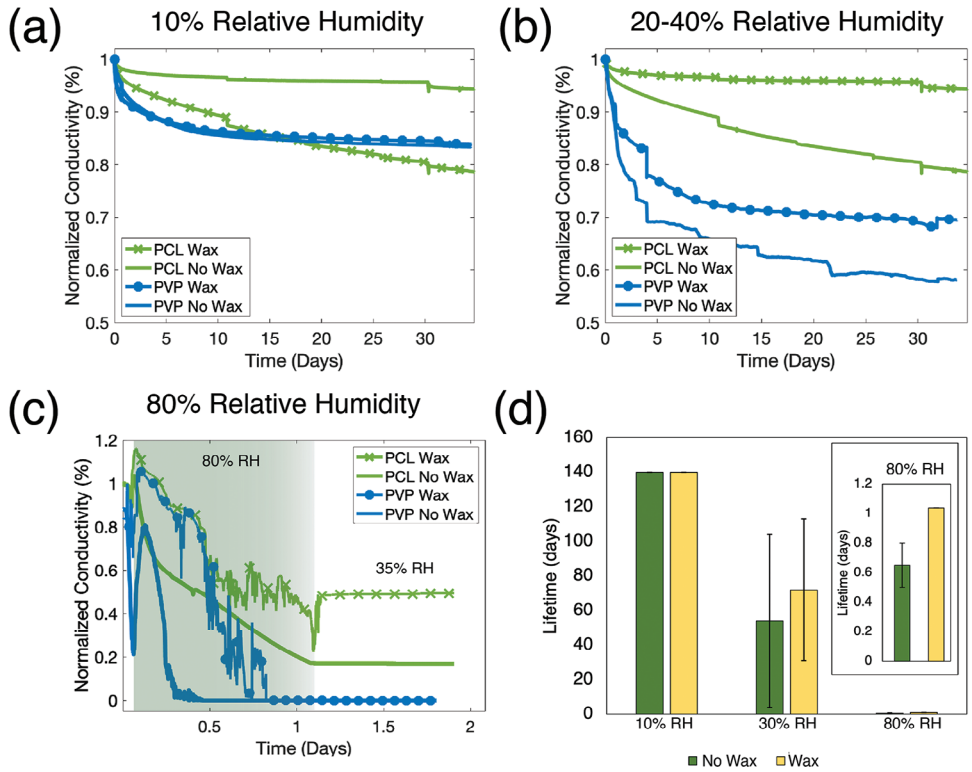

Figure 5. Conductivity over time of zinc traces using PVP binder (blue) and PCL binder (green) with a beeswax coating (symbols) and with no coating (plain lines). a) Samples were kept in an environmental chamber at 19 °C and 10% RH. b) Samples were kept in the lab environment, at about 26 °C and 20–40% RH (environmental data is included in the Supporting Information). c) Samples were exposed to 80%RH for 24 h, then held at 35%RH. d) Lifetime of PCL-based samples under different humidity and encapsulation conditions.

to the ambient laboratory conditions, temperature approximately 26 °C and humidity 20–40% RH, is shown in Figure 5b. The measured temperature and humidity in the lab during this trial is shown in Figure S3 (Supporting Information). Under these conditions, the conductivity of traces with beeswax encapsulation were more stable than those without encapsulation, and all PCL-based traces were more stable than the PVP-based traces. The ambient conditions reported here reflect conditions of one specific lab. Laboratory conditions vary in temperature and humidity levels throughout research institutions, and differences in environmental conditions can impact trace stability.

A separate group of traces was kept in the environmental chamber at 25 °C and 80% RH. The conductivity of those traces over time is shown in Figure 5c. A complete loss of conductivity was observed in PVP-based traces with beeswax encapsulation after 15.9 ± 4.7 (N = 2) hours. In contrast, PVP-based traces without encapsulation failed significantly earlier, after 8.7 ± 4.2 (N = 4) hours. The conductivity of PCL-based traces was more stable than that of PVP-based traces under high humidity levels. After 24 h of exposure to 80% RH, PCL-based trace with encapsulation retained 48% of its initial conductivity, while those without encapsulation retained only 18 ± 1.5% (N = 2) of their initial value. Subsequently, when the chamber humidity was reduced to 35%, the conductivity of PCL-based traces remained unchanged during a 24 h period. For a given binder material, all unencapsulated traces became less conductive more quickly than any of the encapsulated traces.

Further, the conductivity of the PCL-based traces that were kept in low- and moderate- humidity conditions (10% and 30%–40%) was measured over 140 days. Figure S4 (Supporting Information) shows the sheet resistance over the entire test period for these samples. In this study, lifetime is defined as the period of time before the trace's sheet resistance exceeds 0.2 Ω/sq, which is the maximum sheet resistance for the antennas in this study to radiate at least 90% of its input power. Many of the PVP-based samples' initial sheet resistance exceeded this threshold, giving them a useful lifetime of zero days. Figure 5d shows the lifetime of PCL- based samples with and without encapsulation in the three humidity conditions. The longest lifetime of over 140 days was observed for traces kept under 10% humidity. Under ambient lab conditions, the PCL-based trace with beeswax encapsulation had a lifetime of 31 to 113 (N = 3) days, and 4 to 104 (N = 2) days for traces without encapsulation.

High humidity is known to degrade conductivity of printed zinc traces because the water vapor in the air accelerates zinc oxide and hydroxide growth.[18] Sui et al. used a PVP binder and reported an exponential increase in resistance of unencapsulated printed traces over time, with resistance increasing by an order of magnitude after six days in air. Traces encapsulated with wax were reported to maintain 80–85% their conductivity for 30–35 days in air.[10] Majee et al. did not use encapsulation layers and reported conductivity over 250 days. They observed a significant loss of conductivity after 40 days, when humidity in their lab increased.[18] Printed zinc traces intended for outdoor uses will

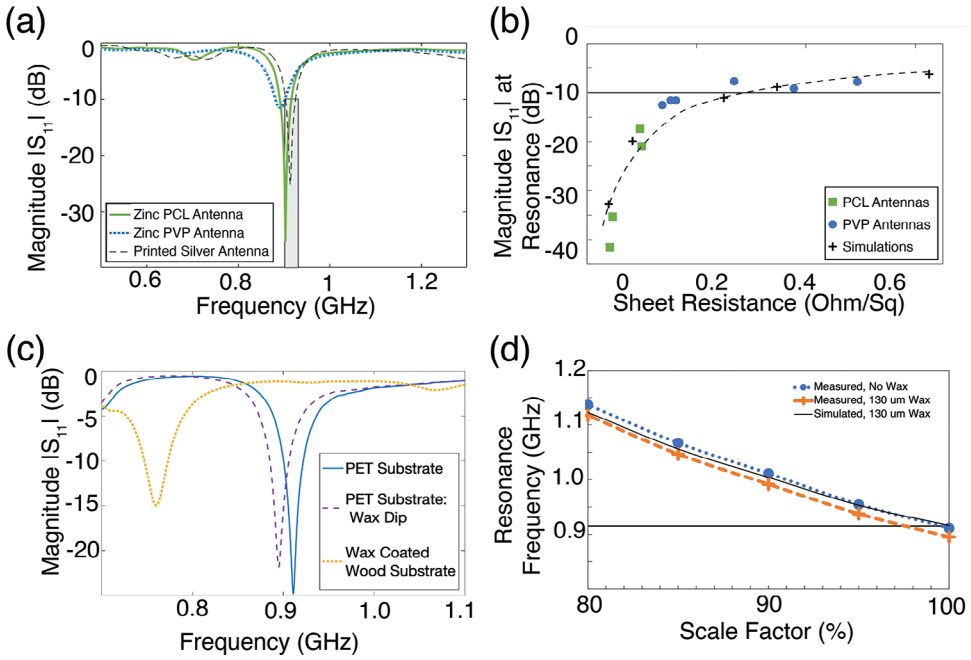

Figure 6. a) Measured S11 parameters for antennas printed on PET substrates. Because PCL-based zinc traces are more conductive, they show a stronger resonance peak than PVP-based zinc antennas. The performance of the PCL-based antennas is comparable to that of antennas printed with commercially available silver ink. b) The depth of the resonance peak is a function of DC sheet resistance. c) A folded dipole antenna had a radiation peak within the 902–927 MHz design band. The same antenna dip coated in 130 µm of beeswax causing the resonance peak to shift to a lower frequency. An antenna printed on a 3 mm wooden substrate with a 200 um wax coating layer has a significantly shifted and reduced resonance peak. d) The relationship between antenna size and resonance frequency for antennas with and without wax layers from simulations and measurement.

need to survive exposure to high heat and humidity over a period of weeks or months. They will rely on encapsulation layers to prolong their functional lifetime.

Additionally, in some environmental conditions, such as in soils, the stability of these traces in liquid water must also be considered. As such, unencapsulated printed traces were also tested in water. The PVP-based trace failed abruptly after about 1.5 hours, while the PCL-based trace remained conductive for more than ten days, as shown in Figure S5 (Supporting Information). In this case, the failure of the trace is driven by dissolution of the binder, rather than slow oxidation of the zinc.

The power reflection coefficient of antennas, S_{11}, fabricated with printed zinc traces was characterized. S_{11} represents the fraction of input power, which is reflected, rather than radiated, when the antenna is attached to a generator with 50Ω impedance. In the resonance band, S_{11} should be less than -10 dB, which means that less than 10% of the power is reflected. **Figure** 6a shows the power reflection coefficient dependence with frequency for PCL-based and PVP-based Zn antennas as prepared (without wax encapsulation on the day they were fabricated). PVP-based antennas show a resonance peak of−10.1 ± 2.1 dB (N = 6), whereas the PCL-based antenna shows a resonance peak of −32.6 ± 10.6 dB (N = 3). For comparison, screen printed silver antennas had a resonance peak of−20.5 ± 2.1 dB (N = 10).

The lower resonance peak of the PVP-based antenna is a result of the lower conductivity and corresponding higher sheet resistance of those traces. The relationship between sheet resistance and $|S_{11}|$ can be seen in Ansys HFSS simulations and measurements. The folded dipole antennas were simulated using bulk conductivity values between 4×10^4 and 6×10^5 Sm^{-1} to represent printed zinc traces, and the trace thickness was 40 µm. Figure S6 (Supporting Information) shows the $|S_{11}|$ simulations as a function of frequency. Figure 6b shows the value of $|S_{11}|$ at resonance as a function of sheet resistance. The relationship between sheet resistance and $|S_{11}|$ is nonlinear. Above 0.2 Ω/*sq*, it is nearly constant, while below this value, $|S_{11}|$ drops quickly with decreasing sheet resistance. The knee at 0.2 Ω/*sq* roughly corresponds to $|S_{11}|$ value of -10 dB, the minimum acceptable value of $|S_{11}|$, which was the value used to define lifetime in Figure 5d. The simulated $|S_{11}|$ values were compared to measured $|S_{11}|$ values of printed zinc antennas made with both PCL and PVP, and the simulated and measured values show good agreement. The sheet resistance of the PVP-based antennas ranged from 0.14 to 0.5 Ω/*sq*. The most conductive PVP-based antennas barely met the design criteria. There was less sample-to-sample variation in sheet resistance of the PCL-based antennas, which ranged from 0.04 to 0.1 Ω/*sq*. This range of sheet resistance values corresponds to a large variation in $|S_{11}|$ because the sheet resistance values are in the range where $|S_{11}|$ is highly dependent on sheet resistance. Importantly, all the PCL-based antennas exceeded the minimum requirements for $|S_{11}|$.

Figure 6c shows power reflection coefficient versus frequency for antennas printed on PET, printed on PET and dip coated with 65 µm of wax on each side, and printed on a wooden substrate with a wax coating. The use of encapsulation layers causes a shift in the resonance frequency, the thicker the wax encapsulation layers are, the greater the measured shift of resonance frequency.

The frequency at which a dipole antenna resonates is described by

$$f = \frac{c\epsilon_r}{2l} \quad (1)$$

where c is the speed of light, ε_r is the relative permittivity of the medium around the dipole, and l the dipole's length. The encapsulation layer around an antenna changes the effective ε_r and thus the resonant frequency of the antenna. Additionally, the depth of the resonance peak is reduced by adding encapsulation layers. Greater losses are observed for thicker wax layers as shown in measurement in Figure 6c, and in simulation in Figure S7 (Supporting Information).

The impact of the encapsulation layer on the resonance frequency can be accounted for by changing l, the physical size of the dipole. In order to quantify the relationship between the physical size of this particular dipole and wax encapsulation layer thickness, antennas of various sizes were printed and their resonance frequency was measured with and without wax encapsulation. A single dip-coated layer of beeswax was 65 µm thick on each side. Simulations of these antennas of different sizes in HFSS with wax layer thicknesses of 130 µm (65 µm front and back), as shown in Figure S5 (Supporting Information) show good agreement with measurements. For this thickness of wax, a folded dipole antenna which is 97%, as large as the original design will resonate at 915 MHz.

3. Conclusion

Chemically treated zinc inks with biodegradable binders can provide the high conductivity needed for functional antennas. The choice of binder material is critical because it sets the limits of the chemical treatment parameters, which in turn determines the conductivity of the printed material. The binder also determines the stability of the resulting printed trace, especially in environments with moisture present. Non-water-soluble PCL withstands higher acid concentrations and exposure times, resulting in higher conductivity, more environmentally stable traces. Beeswax encapsulation layers can protect printed traces from degradation in humid environments, further increasing functional lifetime. Antennas required to operate at a specific frequency must be designed taking this encapsulation layer into account, which can be done by geometric scaling of an existing antenna design.

4. Experimental Section

Zinc Ink Formulation and Printing: To make the inks, PVP, or PCL pellets were dissolved in their corresponding solvent for a few days in a sealed jar at ambient temperature. The PVP was mixed 1:5 by mass in NMP and PCL was mixed 1:8 by mass in NMP or in Anisole. After the polymers had dissolved, powdered zinc (1–5 µm particle size, Goodfellow Co, Pittsburgh, PA) was added at 30:1 by mass to the polymer. The ink was mixed in a planetary mixer for > 30 min prior to printing. All chemicals were procured from Sigma–Aldrich and used as received unless otherwise stated.

Inks were printed with a screen printer using a screen with 325 /in mesh. Printed samples dried in ambient conditions for at least 12 h (NMP-solvent samples) or at least 1 h (Anisole-solvent samples) and profiles were measured with a Dektak MG stylus profilometer (Veeco Instruments, San Jose, CA). Substrates included PET (125 µm thickness), balsa wood (3/16 in thickness, McGuckin Hardwaresource), and poly(3-hydroxybutyrate-co-3-hydroxyvalerate) biopolymer film (PHBV, Goodfellow, 8% valerate content, 0.025 mm thick).

The wood coating process is shown in Figure S8 (Supporting Information). Molten wax was poured on the front of a wooden board of 18 cm by 18 cm and left to cool. A titanium doctor blade (Zehtner ZUA 2000) was heated to >100 °C, then placed on rails such that the final thickness of the wax could be controlled by the height of the blade. The hot blade moved across the wax surface at 10 mms^{-1}, melting and reflowing the wax.

Balsa wood substrates were also prepared by coating a solution of 1:5 PCL: Anisole by mass onto balsa sheets using a doctor blade at room temperature. The coated sheets were then left to dry for a day under ambient conditions, resulting in a 2 µm thick layer of PCL.

Acid Treatment: The samples were laid flat in a tray and a 1-mL syringe was used to deposit about 1 mL of acid solution onto each antenna. The samples were monitored to ensure all printed areas remained covered by solution, and additional solution was added if any areas became exposed. At the end of the allotted time, treatment solution was removed and the samples were transferred to an oven and baked for 15 min.

Encapsulation: White beeswax (Sky Organics, Miami Beach, FL, USA) pellets were melted in a temperature controlled slow cooker at 70 °C. For dip coating, samples were dipped in the molten wax, keeping contact pads exposed, then removed. Layer thickness was measured with calipers.

Longevity Studies: Samples were divided into three groups; one group was kept in an environmental chamber (Associated Environmental Systems, Ayer, MA, USA) held at 19 °C and 10% RH, the second was kept in the uncontrolled lab environment, at about 26 °C and 30–40% RH, and the third was kept in the environmental chamber at to 85% RH and 21 °C for 24 h. With each location, some samples were not encapsulated, and some were dip-coated in beeswax. The resistance of the full 320-mm sample was recorded every minute using a 2-point technique by a multichannel Data Acquisition System (DAQ970A, Keysight Technologies, Santa Rosa, CA). Conditions were monitored with a commercially available temperature and humidity monitor (RH520A, Extech Instruments, Boston, MA, USA).

Antenna Simulation: The folded dipole antennas designs were based on those given in ref. [25] and were modified using numerical simulations in Ansys HFSS 3D Electromagnetic Field Simulator (Ansys, Canonsbur, PA, USA). Zinc ink was simulated with conductivity of 4×10^4, 7×10^4, 1×10^5, 3×10^5, and 6×10^5 Sm^{-1} to represent printed zinc traces, and the trace thickness was 40 µm. The PEN substrate was modeled as a brick with $\varepsilon_r = 3.2$, loss tangent = 0 Sm^{-1}, and thickness = 100 µm, and beeswax layers were modeled with $\varepsilon_r = 2.6$ and loss tangent = 0.07 Sm^{-1}. Simulations used the driven modal mode with a lumped port with Z = 50 Ω. Frequency was swept with 401 points from 456 to 1.37 GHz, centered at 915 MHz. For the smaller geometries, all dimensions, including trace width and gap width, but not the lumped port width, were scaled to fractions of their original size.

Antenna Characterization: Antennas were connected to an SMA cable using SMA connectors friction fit to the printed trace by adding a low density plastic shim behind the sample. Voltage reflection coefficient (S_{11}) measurements of antennas printed using different techniques were executed using a network analyzer (E5061A ENA Series Network Analyzer, Agilent, Santa Clara, CA, USA). Silver antennas used as references were screen printed with silver ink, 126–33 extremely conductive silver ink (Creative Materials, Ayer, MA, USA) and annealed on a hot plate at 130 °C for 10 min.

Supporting Information

Supporting Information is available from the Wiley Online Library or from the author.

Acknowledgements

The authors would like to thank Professor James Evans, from the Materials Science and Engineering, and Dr. Payton Goodrich from Mechanical

Engineering at UC Berkeley for thoughtful discussions. This work was partially supported by the National Science Foundation Graduate Research Fellowships under Grant no. DGE 1752814, and the Advanced Research Projects Agency—Energy award DE-AR0001013. This work was also partially supported by AFRI Competitive Grant no. 2020-67021-32855/project accession no. 1024262 from the USDA National Institute of Food and Agriculture. This grant is being administered through AIFS: the AI Institute for Next Generation Food Systems. https://aifs.ucdavis.edu.

Conflict of Interest

The authors declare no conflict of interest.

Data Availability Statement

The data that support the findings of this study are available from the corresponding author upon reasonable request.

Keywords

low temperature processing, RFID, transient antennas, transient conductors, transient electronics, zinc

Received: September 22, 2023
Revised: December 20, 2023
Published online:

[1] N. Ashammakhi, A. L. Hernandez, B. D. Unluturk, S. A. Quintero, N. R. de Barros, E. Hoque Apu, A. Bin Shams, S. Ostrovidov, J. Li, C. Contag, A. S. Gomes, M. Holgado, *Adv. Funct. Mater.* **2021**, *31*, 2104149.
[2] W. Tian, Y. Li, J. Zhou, T. Wang, R. Zhang, J. Cao, M. Luo, N. Li, N. Zhang, H. Gong, J. Zhang, L. Xie, B. Kong, *ACS Appl. Mater. Interfaces* **2021**, *13*, 8285.
[3] M. Rüegg, R. Blum, G. Boero, J. Brugger, M. Rüegg, R. Blum, G. Boero, J. Brugger, *Adv. Funct. Mater.* **2019**, *29*, 1903051.
[4] J. S. Shim, J. A. Rogers, S. K. Kang, *Mater. Sci. Eng.: R: Rep.* **2021**, *145*, 100624.
[5] W. B. Han, S. M. Yang, K. Rajaram, S. W. Hwang, *Adv. Sustainable Syst.* **2022**, *6*, 2.
[6] Y. Li, Q. Yang, M. Chen, M. Wang, M. Zhang, *Sensors (Switzerland)* **2019**, *19*, 21.
[7] S. S. Sethi, M. Kovac, F. Wiesemüller, A. Miriyev, C. M. Boutry, *Nat. Ecol, Evol.* **2022**, *6*, 1245.
[8] Y. K. Lee, J. Kim, Y. Kim, J. W. Kwak, Y. Yoon, J. A. Rogers, *Adv. Mater.* **2017**, *29*, 38.
[9] S. Feng, Z. Tian, J. Wang, S. Cao, D. Kong, *Adv. Electron. Mater.* **2019**, *5*, 3.
[10] Y. Sui, A. N. Radwan, A. Gopalakrishnan, K. Dikshit, C. J. Bruns, C. A. Zorman, G. L. Whiting, *Adv. Eng. Mater.* **2022**, *35*, 2200529.
[11] S. L. Merilampi, T. Bjorninen, A. Vuorimaki, L. Ukkonen, P. Ruuskanen, L. Sydanheimo, *Proc. IEEE* **2010**, *98*, 1610.
[12] P. Pongpaibool, in *International Symposium on Antennas and Propagation*, IEEE, Nagoya, Japan **2012**, pp. 1248–1251.
[13] M. Shahpari, D. V. Thiel, *IEEE Trans. Antennas Propag.* **2015**, *63*, 4686.
[14] L. V. Kayser, D. J. Lipomi, *Adv. Mater.* **2019**, *31*, 1806133.
[15] J. Li, H. Xu, Z. Zhang, Y. Hao, H. Wang, X. Huang, J. Li, H. Xu, Z. Zhang, X. Huang, Y. Hao, H. Wang, *Adv. Funct. Mater.* **2020**, *30*, 1905024.
[16] B. K. Mahajan, X. Yu, W. Shou, H. Pan, X. Huang, B. K. Mahajan, X. Yu, W. Shou, H. Pan, X. Huang, *Small* **2017**, *13*, 1700065.
[17] N. Fumeaux, D. Briand, *npj Flexible Electron.* **2023**, *7*, 1.
[18] S. Majee, M. C. Karlsson, A. Sawatdee, M. Y. Mulla, N. u. H. Alvi, V. Beni, D. Nilsson, *npj Flexible Electron.* **2021**, *5*, 1.
[19] S. Feng, Z. Tian, J. Wang, S. Cao, D. Kong, *Adv. Electron. Mater.* **2019**, *5*, 1800693.
[20] H. Almasi, M. Jahanbakhsh Oskouie, A. Saleh, *Crit. Rev. Food Sci. Nutr.* **2021**, *61*, 15.
[21] M. Mantecón-Oria, N. Diban, M. T. Berciano, M. J. Rivero, O. David, M. Lafarga, O. Tapia, A. Urtiaga, *Membranes* **2020**, *10*, 8.
[22] E. Malikmammadov, T. Endogan Tanir, A. Kiziltay, V. Hasirci, N. Hasirci, *J. Biomater. Sci.* **2018**, *29*, 863.
[23] K. Krasowska, A. Heimowska, M. Morawska, in *E3S Web of Conferences* **2016**, *10*, 00048.
[24] B. C. Almeida, P. Figueiredo, A. T. Carvalho, *ACS Omega* **2019**, *4*, 6769.
[25] C. Baumbauer, M. Anderson, J. Ting, A. Sreekumar, J. Rabaey, A. Arias, A. Thielens, *Sci. Rep.* **2020**, *10*, 1.
[26] K. Jayasayee, S. Clark, C. King, P. I. Dahl, J. R. Tolchard, M. Juel, *Processes* **2020**, *8*, 5.
[27] M. Atreya, G. Marinick, C. Baumbauer, K. V. Dikshit, S. Liu, C. Bellerjeau, J. Nielson, S. Khorchidian, A. Palmgren, Y. Sui, R. Bardgett, D. Baumbauer, C. J. Bruns, J. C. Neff, A. C. Arias, G. L. Whiting, *ACS Appl. Electron. Mater* **2022**, *4*, 4920.
[28] J. Bourely, L. De Sousa, N. Fumeaux, O. Vorobyov, C. Beyer, D. Briand, *Micro Nano Eng.* **2023**, *19*, 100185.
[29] N. Fumeaux, M. Kossairi, J. Bourely, D. Briand, *Micro Nano Eng.* **2023**, *20*, 100218.
[30] L. Van Der Schueren, B. De Schoenmaker, Ö. I. Kalaoglu, K. De Clerck, *Eur. Polym. J.* **2011**, *47*, 1256.
[31] P. Bordes, E. Pollet, L. Avérous, *Prog. Polym. Sci.* **2009**, *34*, 125.
[32] M. B. Atreya, Design of Additively Fabricated Biodegradable Sensors for Soil Monitoring, Ph.D. thesis, University of Colorado Boulder, Boulder, CO, **2022**.